Amplification of Local Interactions

Thermally Induced Electron Transfer in a CsCoFe Prussian Blue Derivative: The Specific Role of the Alkali-Metal Ion**

Anne Bleuzen, Virginie Escax, Alban Ferrier,*
Françoise Villain, Michel Verdaguer, Pascal Münsch,
and Jean-Paul Itié

Prussian blue was described for the first time in 1704. Since then, spectacular electrochemical,[1,2] magnetic,[3,4] and photomagnetic[5] properties have been revealed in Prussian blue analogues, all of which revived interest in their study. These compounds crystallize in face-centered cubic (fcc) structures. Insertion of alkali metal ions in the tetrahedral sites (Td) is accompanied by a change in stoichiometry.[6,7] Several recent studies pointed out the role played by the inserted alkali metal ions for the properties of the Prussian blue analogues.[2,7,8] Here we focus on the role of cesium in the thermally activated electron transfer Co^{II}(high spin)-$Fe^{III} \rightarrow Co^{III}$(low spin)-$Fe^{II}$ in the derivative $Cs_{0.7}Co_4[Fe(CN)_6]_{2.9}\square_{1.1}\cdot 16\,H_2O$ (**$Cs_{0.7}$**; $\square$ represents the intrinsic $[Fe(CN)_6]$ vacancies). We chose this specific stoichiometry since its most probable Td-site environment is $Co_4Fe_3\square_1$. The electron transfer occurs over the temperature range 280–180 K.[7] In **$Cs_{0.7}$**, the Co^{III}/Co^{II} ratio is 9:1 at room temperature and 3:2 at 20 K.[7,9] The study of the local environment of the metal ions (by X-ray absorption spectroscopy) and of the long-range order (by powder energy-dispersive X-ray diffraction) made it possible for the first time to localize the alkali metal cations in the structure, to demonstrate specific interactions between them and the bimetallic network, and to determine a displacement of them in the cavities between room and low temperatures.

Extended X-ray absorption fine structure (EXAFS) measurements were performed at the Fe and Co K-edges at 300 and 20 K. The $[Fe(CN)_6]$ entity is stable and rigid. The EXAFS signals at the Fe K-edge at 300 and 20 K are therefore very close to each other.[10] In contrast, at the Co K-edge, the EXAFS signals are very different at 300 and 20 K (Figure 1).

---

[*] Dr. A. Bleuzen, Dr. V. Escax, A. Ferrier, Dr. F. Villain,
Prof. Dr. M. Verdaguer
Laboratoire de Chimie Inorganique et Matériaux Moléculaires
UMR CNRS 7071, Université Pierre et Marie Curie
Bat F, 4, place Jussieu, 75252 Paris Cedex 05 (France)
Fax: (+33) 144-273-841
E-mail: bleuzen@ccr.jussieu.fr

Dr. P. Münsch, Dr. J.-P. Itié
Laboratoire pour L'Utilisation du Rayonnement Electromagnétique
UMR CNRS 130-CEA-MENRS
Bat 209d, Université Paris Sud
BP34, 91898 Orsay Cedex (France)

[**] This research was supported by the DFG (Schwerpunktprogramm 1137: Molekularer Magnetismus), the European Community (TMR Programme), and MENESR (grant for V.E.).

Supporting information for this article is available on the WWW under http://www.angewandte.org or from the author.

DOI: 10.1002/ange.200460086

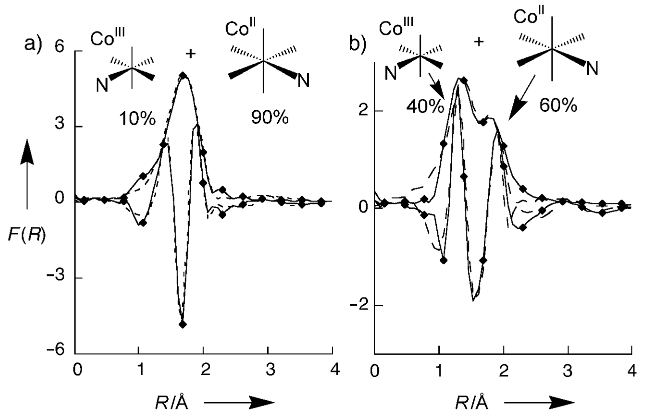

Figure 1. Experimental (——) and calculated (– – –) modulus and imaginary parts of the first-neighbor contributions to the Fourier transform of the EXAFS signal at the Co K-edge of **Cs$_{0.7}$** a) at 300 K and b) at 20 K.

The data analysis at 300 K shows the presence of 5.4 N or O at 2.09(3) Å (corresponding to 90 % octahedrally coordinated Co^{II}(HS)) and 0.6 N or O at 1.90(3) Å (corresponding to 10 % Co^{III}(LS)). At 20 K, we find 3.6 N or O at 2.08(3) Å (60 % Co^{II}(HS)) and 2.4 N or O at 1.89(3) Å (40 % Co^{III}(LS)).[7,9]

Powder energy-dispersive X-ray diffraction (EDX) spectra of **Cs$_{0.7}$** were recorded as a function of temperature on cooling from 300 to 140 K. At 300 K, the diffraction pattern of **Cs$_{0.7}$** can be indexed to a fcc unit cell. On cooling, the area and the linewidth of the peaks do not vary significantly (Figure 2), whereas all the diffraction lines shift progressively towards higher energy, corresponding to a progressive decrease of the cell parameter from 10.30(5) Å at 300 K to 10.08(5) Å at 140 K. This cell contraction is due to the shortening of the Co–ligand bond accompanying the Co^{II}(HS)→Co^{III}(LS) transformation. These observations correspond to a second-order transformation which starts locally and spreads homogeneously in the solid without loss of crystallinity.[11]

EXAFS measurements were also performed at the Cs L$_3$-edge at 300 and 20 K (Figure 3). At 300 K, the Fourier transform of the EXAFS signal of **Cs$_{0.7}$** exhibits well-defined contributions: the Cs ion has rather strong interactions with its neighbors. The first contribution to the Fourier transform is well simulated by three O and six N atoms situated 3.46(5) Å from the Cs ion. A coordination number of nine is sensible for a cation of this size and charge.[12] The second shell is well simulated by 6 C atoms situated at 3.72(5) Å, while the third and fourth ones are well simulated by three Co and three Fe atoms situated at 4.37(5) Å and 5.05(5) Å, respectively. The four well-resolved shells and the distances obtained clearly indicate that the Cs ion is not situated at the center of the Td site. The vacancy □, the center of the Td site, and—for symmetry reasons—the Cs ion are situated on a threefold axis (see Figure 3 a).

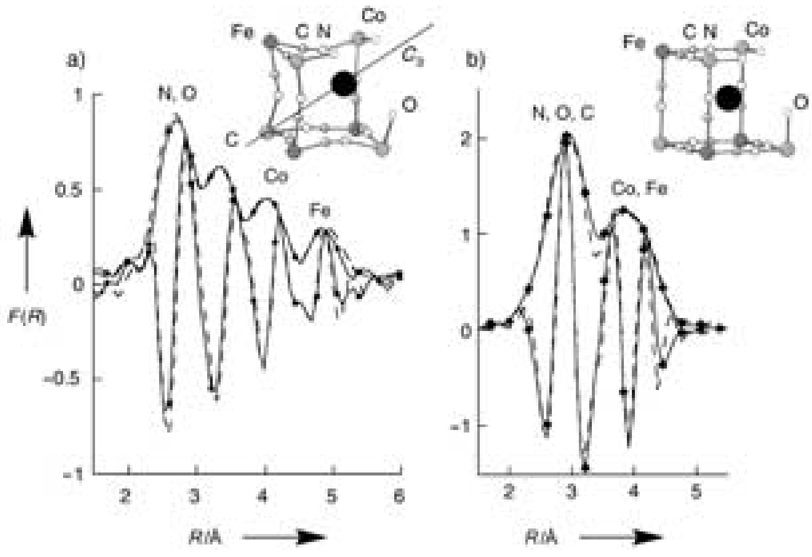

Figure 3. Experimental (——) and calculated (– – –) modulus and imaginary parts of the first-neighbor contributions to the Fourier transform of the EXAFS signal at the Cs L$_3$-edge of **Cs$_{0.7}$** and schematic presentation of the Cs environment a) at 300 K and b) at 20 K.

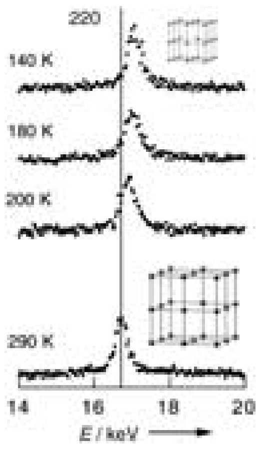

Figure 2. EDX spectra of **Cs$_{0.7}$** between 14 and 20 keV [(220) diffraction line] as a function of temperature.

From the Cs–Fe and Cs–Co distances and from the cell parameters, it is easy to localize the Cs ion on the threefold axis at about 1 Å from the center of the Td site towards the vacancy. Taking an Fe–C distance as 1.93 Å,[10] it is possible to calculate from X-ray diffraction and absorption data the coordinates of the Cs, C, N, Co, and Fe atoms in the plane containing the Co, Fe, and Cs metal ions and the CN bridge interacting with them (CoFeCs plane). The positions of the atoms are shown in Figure 4.[13] The Co–NC entity is bent.[14,15] A schematic drawing of the environment of the Cs ion is given Figure 3 a.

At 20 K, only two shells of neighboring atoms can be extracted from the Fourier transform of the EXAFS signal of **Cs$_{0.7}$**. The first one is well simulated by 21 O, N, or C atoms situated at 3.55(5) Å and the second one by 7 Co or Fe atoms located 4.30(5) Å from the Cs ion. The Cs ion is located at the center of the Td site at equal distances from the Co and Fe

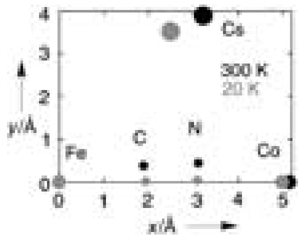

Figure 4. Position of the Co, Fe, C, N, and Cs atoms in the CoFeCs plane at 300 K (black circles), and at 20 K (gray circles).

ions.[16] Taking an Fe–C distance of 1.93 Å,[10] we calculated the coordinates of the different atoms in the CoFeCs plane from the 20-K EXAFS data. A schematic drawing of the environment of the Cs ion and the calculated positions for a Co^{III}–N distance of 1.89 Å are shown in Figure 3b and 4, respectively.[13] There is no sensible solution for the coordinates of the N atom with a Co^{II}–N distance of 2.08 Å. The EXAFS data at the Cs L_3-edge are not compatible with a structure in which Co^{II}(HS) would be the closest Co neighbors.[17] At 20 K, the Cs ions are surrounded exclusively by Co^{III}(LS) ions and linear Co-NC-Fe entities. Furthermore, since the number of Co ions undergoing an oxidation-state change on cooling (30%) corresponds exactly to the number of Co ions surrounding the Cs ion,[18] one might conclude that only these Co ions are involved in the electron transfer. Thus, the presence of the Cs ion appears as a condition for the electron transfer.

This structural investigation shows that in $\mathbf{Cs_{0.7}}$ the electron transfer occurs only around the Td sites containing a Cs ion. At 300 K, the Cs ion is surrounded by Co^{II} and Fe^{III} ions (see Figure 3a). It is displaced from the center of the Td site and interacts with the O atoms of three H_2O molecules, which are bound to the three Co ions neighboring the vacancy, and with the six nearest CN bridges. The Co^{II}-NC-Fe^{III} entities are bent. The orbital interactions between Co and NC are weak (compared to those in the linear conformation). The ligand field of Co is weak, the Co ions are HS at the oxidation state +II. $\mathbf{Cs_{0.7}}$ is essentially composed of Co^{II} and Fe^{III} ions. The Cs ion fits into the CoFe bimetallic network to complete its coordination sphere with nine neighbors. The crystal and electronic structures of $\mathbf{Cs_{0.7}}$ are close to those of the CoFe Prussian blue analogue free of the alkali metal ion.

At low temperature, the alkali metal ions move to the center of the Td sites and interact with all the ligands surrounding this site (nine CN bridges and three H_2O molecules). The Co^{III}-NC-Fe entities become linear. The orbital interactions between Co and NC are stronger and so is the Co ligand field. The Co ions around the alkali metal ion are LS at the oxidation state +III. $\mathbf{Cs_{0.7}}$ is still mainly composed of Co^{II} ions (60%) except around the alkali metal ion. The cell parameters are shortened due to the formation of linear Co^{III}-NC-Fe entities around the alkali metal ions. As shown by the absence of loss of crystallinity in the sample, the structural change spreads in a cooperative way in the whole solid, made possible by the flexibility of the Co-NC angle in the Co^{II}-NC-Fe entities and by the swing of the Co and Fe coordination polyhedra.

The high- and low-temperature states of $\mathbf{Cs_{0.7}}$ are close in energy, with a lower entropy in the more rigid low-temperature state. The switching process is reversible, thermally (and entropy-) driven in line with the observations by Sorai and Seki about the coupling between electronic states and phonons.[21] It is accompanied by a move of the alkali metal ion and by an electron transfer. Our finding is related to the very peculiar structural role of the alkali metal ion in the process: it fits into the CoFe bimetallic network at 300 K, moves to the center of the Td site, and modifies the structure around it at low temperature. Such geometry changes were already observed in perovskite oxides, where they were imposed by interactions between lanthanide ions and oxo bridges and associated with changes in some properties.[19] What is spectacular in the CoFe Prussian blue analogues is the macroscopic influence of local interactions on the network as a consequence of their amplification by electron transfer and Co-spin change. Work is in progress on other Prussian blue analogues, at both structural and electronic levels (in particular to determine the ligand field of the cobalt ions), to check the general existence of such interactions in these analogues.

Experimental Section

The synthesis of $\mathbf{Cs_{0.7}}$ is described in ref. [7].

The EXAFS measurements were carried out in transmission mode on the XAS 13 beamline at LURE (Orsay) and the signals were calculated in the single-scattering approximation.[20]

EDX patterns were recorded on the DW-11A energy-dispersive X-ray beamline at LURE (Orsay).[11] The photoexcitation of the sample under the X-ray beam prevented us from recording EDX spectra at temperatures below 140 K. XAS data parameters of the calculated spectra and calculation of the atomic coordinates are available in the Supporting Information.

Received: March 22, 2004 [Z460086]

Keywords: electron transfer · Prussian blue analogues · spin crossover · X-ray absorption spectroscopy · X-ray diffraction

---

[1] K. Honda, J. Ochiachi, H. Hayashi, *Chem. Commun.* **1986**, 168–170.

[2] D. R. Rosseinsky, H. Lim, X. Zhang, H. Jiang, J. Wei Chai, *Chem. Commun.* **2002**, 2988–2989.

[3] T. Mallah, S. Thiébault, M. Verdaguer, P. Veillet, *Science* **1993**, *262*, 1554–1557.

[4] a) S. Ferlay, T. Mallah, R. Ouahès, P. Veillet, M. Verdaguer, *Nature* **1995**, *378*, 701–703; b) S. M. Holmes, G. S. Girolami, *J. Am. Chem. Soc.* **1999**, *121*, 5593–5594; c) N. Shimamoto, O. Ohkoshi, O. Sato, K. Hashimoto, *Inorg. Chem.* **2002**, *41*, 678–684.

[5] O. Sato, T. Iyoda, A. Fujishima, K. Hashimoto, *Science* **1996**, *272*, 704–705.

[6] A. Lüdi, H. U. Güdel, *Structure and Bonding*, Springer, Berlin, **1973**, pp. 1–21.

[7] V. Escax, A. Bleuzen, C. Cartier dit Moulin, F. Villain, A. Goujon, F. Varret, M. Verdaguer, *J. Am. Chem. Soc.* **2001**, *123*, 12536–12543.

[8] a) J. J. Garcia-Jareno, A. Sanmatias, J. Navarro-Laboulais, F. Vicente, *Electrochim. Acta* **1998**, *43*, 395–405; b) J. J. Garcia-

Jareno, J. Navarro-Laboulais, A. Sanmatias, F. Vicente, *Electrochim. Acta* **1998**, *43*, 1045–1052.

[9] A. Bleuzen, V. Escax, J.-P. Itié, P. Münsch, M. Verdaguer, *C. R. Chim.* **2003**, *6*, 343–352.

[10] T. Yokoyama, T. Ohta, O. Sato, K. Hashimoto, *Phys. Rev. B* **1998**, *58*, 8257–8266.

[11] V. Escax, A. Bleuzen, J. P. Itié, P. Münsch, F. Varret, M. Verdaguer, *J. Phys. Chem. B* **2003**, *107*, 4763–4767.

[12] H. Ohtaki, T. Radnai, *Chem. Rev.* **1993**, *93*, 1157–1204.

[13] The C–N distance in the CN bridge calculated from the calculated coordinates is 1.2(1) Å at 300 K and 1.1(1) Å at 20 K, and thus of the expected order of magnitude (1.14 Å).

[14] K. H. Hallmeier, S. Sauter, R. Szargan, *Inorg. Chem. Commun.* **2001**, *4*, 153–156.

[15] R. Garde, F. Villain, M. Verdaguer, *J. Am. Chem. Soc.* **2002**, *124*, 10531–10538.

[16] T. Yokoyama, H. Tokoro, S.-I. Ohkoshi, K. Hashimoto, K. Okamoto, T. Ohta, *Phys. Rev. B* **2002**, *66*, 184111–184111-20.

[17] Furthermore, for a Co^{II} ion and a necessarily bent Co^{II}-NC-Fe entity around the Cs ion, or for a mixture of this environment and the linear Co^{III}-NC-Fe entity, the calculated EXAFS signal is completely different from the experimental one.

[18] The number of Co atoms per unit cell surrounding one Td site is $(1+{}^{3}/_{4})$. As the Cs ions are diluted in the structure (0.7 per unit cell), the number of Co atoms surrounding one Cs ion is given by $0.7\times(1+{}^{3}/_{4})$, which corresponds to 30 % of the Co ions.

[19] P. Lacorre, J. B. Torrance, J. Pannetier, A. Nazzal, P. W. Wang, T. C. Huang, *J. Solid State Chem.* **1991**, *91*, 225–237.

[20] C. Cartier dit Moulin, F. Villain, A. Bleuzen, M.-A. Arrio, P. Sainctavit, C. Lomenech, V. Escax, F. Baudelet, E. Dartyge, J. J. Gallet, M. Verdaguer, *J. Am. Chem. Soc.* **2000**, *122*, 6653–6658.

[21] M. Sorai, S. Seki, *J. Phys. Chem. Solids* **1974**, *35*, 555–570.